Journal of Electron Devices, Vol. 19, 2014, pp. 1642-1647

© JED [ISSN: 1682 -3427]

Journal of Electron Devices
www.jeldev.org

WIDE BANDGAP, p-TYPE SEMICONDUCTING SnO THIN FILM GROWN BY PULSED LASER DEPOSITION

Saritha A.C[a]*, Sasanka Kumar S[a], Majeesh M[a], Hasna K[a,b], Subha P.P[a], Vikas L.S[a], M.K. Jayaraj[a,c]

[a] Department of Physics, Cochin University of Science and Technology , Kochi 682 022, India

[b] Department of Instrumentation, Cochin University of Science and Technology , Kochi 682 022, India

[c] Centre for advanced materials, Cochin University of Science and Technology , Kochi 682 022, India

sarithaac@gmail.com

Received 24-03-2014, online 31-03-2014

ABSTRACT

Transparent SnO thin films with *p*-type conductivity were grown on glass substrate by PLD at room temperature (RT) followed by an annealing at 400^0C in oxygen ambience. For the deposition of SnO thin film from a metallic Sn target, control over the oxygen partial pressure (PO_2) and substrate temperature during deposition and annealing was very critical. The obtained SnO_x films were studied systematically using grazing incidence x-ray diffraction, Raman spectroscopy, X-ray photoelectron spectroscopy, atomic force microscopy, UV-Vis-NIR spectroscopy and Hall-effect measurement. Hall measurements of SnO film gave a maximum hole concentration ~10^{17} cm^{-3} and a hole mobility of 2.8 $cm^2V^{-1}s^{-1}$. The transparency of the SnO film in the visible region was only 50%. A direct band gap of 2.93eV was found from the Tauc plot. AFM measurement showed that the film surface has a roughness of 19 nm which is not suitable for device fabrication.

Keywords: *p*-type TOS; SnO thin film; PLD; GIXRD; Raman analysis; Hall measurement.

I. INTRODUCTION

Interest in p-type transparent oxide semiconductors (TOS) has rapidly grown in recent years due primarily to strong demand for bipolar optoelectronic devices such as light-emitting diodes, laser diodes, solar cells, thin film transistors (TFTs) etc. Although many *n*-type TOSs with superior performance are in extensive use [1-3], high quality wide bandgap oxides exhibiting p-type conductivity remain few [4-6]. This confines the field of application of oxide semiconductors solely to unipolar (n-type) devices, inhibiting the fabrication of complementary metal oxide semiconductor (CMOS) based devices. In general the valence band maxima (VBM) of oxide semiconductors are mainly formed from localized and anisotropic O 2p orbitals, which lead to a low hole mobility due to a percolation/hopping conduction. Therefore a modulation of the energy band structure to reduce the localization of the valence band edge was of primary importance in the chemical design of *p*-type conductive wide gap ionic solids in early days. The cationic species was required to have a closed shell whose energy is almost comparable to those of the 2p levels of oxygen anions. Based on this theory many p-type transparent oxide semiconductors, such as $CuAO_2$ (A=B, Al, Ga, and In), $SrCu_2O_2$, and LaCuOCh (CH=S and Se) were discovered by making use of the hybridization between O 2p and Cu 3d orbitals [4, 5]. Later on, consideration of a different hole transport path which is made of spatially spread s-orbitals lead to the finding of a new *p*-type oxide semiconductor; tin monoxide (SnO), with a large hole mobility [7].

SnO, which is an important oxide phase of the tin-oxygen system possess a wide band gap ranging from 2.5eV to 3.3 eV [8]. The higher energy region of SnO contains Sn 5s, Sn 5p, and O 2p components nearly equally. The valence band is formed by hybridized orbitals of O 2p and Sn 5s [9]. But very near the VBM the contribution of Sn 5s is dominant than the relatively small O 2p component and this helps in reducing the localization of the valence band edge and enhance the hole mobility. As a result of this configuration SnO shows excellent *p*-type behaviour making it an interesting candidate for many optoelectronic applications, including *p* channel TFTs and complimentary circuits. Many research groups have realised heterojunction diodes [10] and TFTs

[9, 11] with fine performance using SnO as the *p* layer.

Various techniques such as electron beam evaporation, chemical vapor deposition, aqueous solution process, hydrothermal synthesis, magnetron sputtering etc are in widespread use for the deposition of SnO thin films , but only two groups have reported the pulsed laser deposition of SnO thin films. [9,12]. The first report by Fan and Reid [12] was mainly focused not on SnO film, but on SnO_2 film from a SnO_2 target by PLD using a wavelength 532nm.Ogo *et al* [9], for the first time, reported the deposition of *p*-type SnO film by PLD from a ceramic SnO target for TFT application. The substrate was YSZ kept at a temperature of 575^0C and the ablation source was KrF Excimer laser operating at a wavelength of 248 nm. Irrespective of the deposition technique, it is generally observed that low values of substrate temperature (Ts) and oxygen partial pressure (Po_2) during deposition and annealing leads to a mixed β-Sn and α-SnO phase formation in the film whereas SnO_2 phase is obtained at elevated values of these parameters. Moreover SnO is less stable compared to SnO_2 and always shows a tendency to transform to the stable SnO_2 phase. Hence the optimum growth conditions for SnO thin film are exceptionally narrow, especially in PLD, where the plume dynamics is extremely complex and nonuniform.

In this paper, the growth of p-type SnO_x thin film that exhibits a hall mobility of 2.8 $cm^2V^{-1}s^{-1}$ and a hole concentration ~10^{17} cm^{-3}, by PLD using a wavelength of 355 nm, is reported. The transparency of the SnO film in the visible region was found to be only 50%. Even though low-temperature processed oxide films are preferred for practical device applications, deposition at room temperature (RT) under controlled oxygen partial pressure and a high temperature (400^0C) annealing processes were examined in this study, enabling growth of SnO film on low cost glass substrate. The structural, compositional, optical, electrical and morphological properties of the films are comprehensively investigated.

II. EXPERIMENTAL

The deposition was carried out using the third harmonics (λ=355 nm) from a Q-switched Nd: YAG (Yttrium Aluminium Garnet) laser (Quanta Ray, Spectra Physics, GCR 150) having a pulse width of 8 ns, and repetition frequency of 10 Hz. The target (high purity Sn foil) was mounted inside a stainless steel vacuum chamber which was evacuated to a base pressure of $4x10^{-6}$ mbar. The laser beam was focused onto the rotating target using a quartz lens with focal length f =30 cm at an angle of 45° with respect to the target normal. The spot size of the laser was adjusted to be 1 mm diameter and hence the laser fluence was 2.5 J /cm^2.The distance between the substrate and the target was kept fixed at 6 cm. The flow of oxygen into the chamber was controlled through an oxygen mass flow controller. The schematic of the PLD system is shown in Figure 1.

Compared to other thin film growth techniques, the advantage of PLD is that highly crystalline films can be grown even at lower substrate temperature. In this work the films were deposited on the glass substrate which is kept at room temperature (T_s = 25^0C) under different oxygen pressures (Po_2) ranging from 0.001 mbar to 0.1 mbar and further annealed in oxygen ambience at 0.1 mbar at temperatures 200^0C, 400^0C and 600^0C to optimize the SnO growth condition.

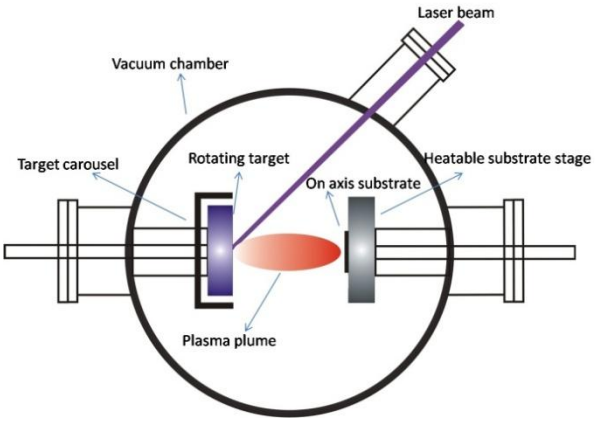

Figure 1: Schematic of PLD system

The phase composition of the films was characterized by grazing incidence x-ray diffraction (GIXRD) using PANalytical X'Pert PRO with Cu-Kα radiation (λ= 1.5418Å). The microstructure was elucidated by analyzing the Raman spectra recorded using Lab RAM HR spectrophotometer (HORIBA JOBIN YVON) with Ar ion laser (514.5nm) as the excitation source. X-ray photoelectron spectroscopy (XPS) measurements were used to perform compositional analysis. The thickness of the film was measured by a stylus surface profiler (Dektak 6 M). Jasco V-570 UV-VIS-NIR spectrophotometer was used to record the transmission spectra. Carrier transport

properties were examined by Hall-effect measurement in the Van Ber Pauw configuration. Surface morphology of the film was studied by Agilent 5500 series atomic force microscope (AFM) in non contact mode.

III. RESULTS AND DISCUSSIONS

The structural and electrical properties of the SnO_x films is found to show three distinct regions: viz, as deposited polycrystalline film with mixed β-Sn and α-SnO phases which is highly resistive; 400^0C annealed α-SnO phase dominated film with *p*-type conductivity and 600^0C annealed SnO_2 phase dominated films with *n*-type conductivity.

As can be seen from the XRD θ-2θ scans of as deposited films under vacuum and different O_2 pressures (Figure 2), oxygen gas plays an important role in modifying the properties of the as deposited films. A low O_2 pressure results in growth of metallic tin film. On increasing the oxygen pressure to 0.01 mbar, the Sn peak at 30.6^0 (200 reflection) broadens (position marked*) because of its possible merging with the α-SnO peak at 29.9^0 (101 reflection). This is confirmed from the observation that further increase in pressure to 0.1 mbar resulted in a film with a small trace of SnO_2 (position marked ▪). The presence of α-SnO phase in the as deposited film has been detected in the Raman spectrum also. So deposition at 0.01mbar O_2 pressures is found to be more suitable for α-SnO phase formation.

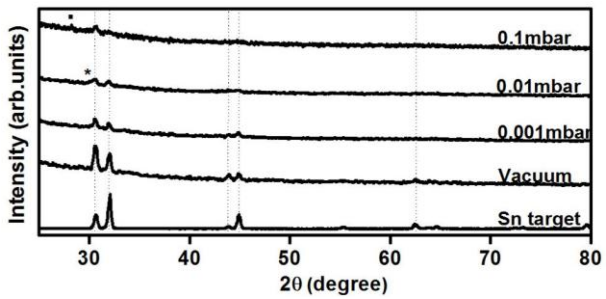

Figure 2: XRD θ-2θ scans of as deposited films under vacuum and different O_2 pressures

III.1 Structural Properties

III.1.1 XRD Measurements:

Figure 3 shows the GIXRD patterns of the as deposited and annealed films along with that of the tin target. In the as deposited film (Ts=25^0C, Po_2= 0.01mbar) only Sn peaks were observed (ICSD#:040038) with traces of SnO phase. Annealing was performed at temperatures 200^0C, 400^0C and 600^0C keeping Po_2 = 0.1mbar inside the chamber. 200^0C annealing gave an indication of the formation of crystalline α-SnO phase. Annealing of the as deposited film at 400^0C resulted in α-SnO phase, but with some traces of metallic Sn. As temperature increased to 600^0C the α-SnO and Sn peaks disappeared completely resulting in a pure SnO_2 phase.

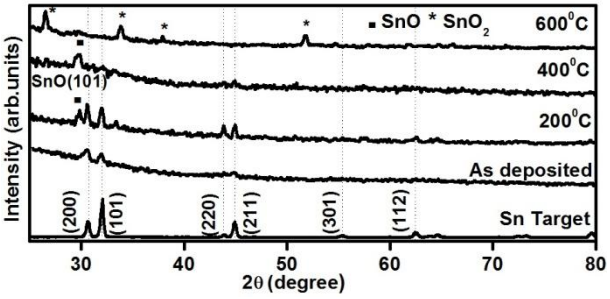

Figure 3: XRD θ-2θ scans of as deposited and annealed films along with that of Sn target

The peak located at 29.9^0 in the 400^0C annealed film corresponds to the (101) plane of the tetragonal α-SnO phase (space group P4/nmm). Even though the α-SnO peak has a low intensity no peaks from SnO_2 or any other impurity phases were observed within the instrumental detection limit.

III.1.2 Raman Measurements:

Raman active phonon modes of the films were identified by the micro Raman measurements. As observed in the GIXRD, Raman spectra [Figure 4] also show the presence of SnO phase in the as deposited films. Only two peaks located at 112 and 211 cm^{-1} were observed for the film annealed at 400^0C which are the characteristic B_{1g} and A_{1g} vibrational modes of SnO [13]. Characteristic peaks of SnO_2 at 471 cm^{-1} (E_g), 632 cm^{-1} (A_{2g}) and 773 cm^{-1} (B_{2g}) [14] are absent in the Raman spectra obtained for this film, which indicate that film is purely SnO phase. Annealing temperature of 600^0C resulted only in the tetragonal phase of SnO_2.

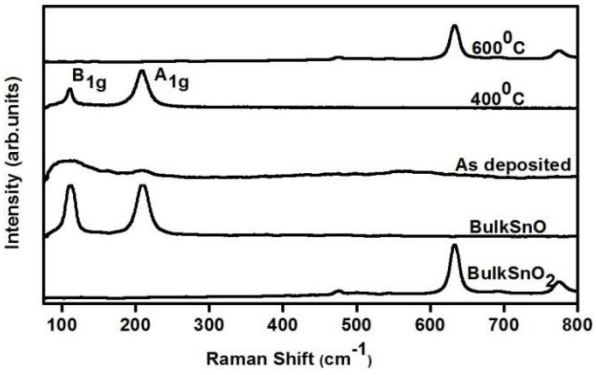

Figure 4: Raman spectrum of as deposited and annealed films along with bulk samples

III.2. Compositional Properties

XPS survey scan spectrum of the film is shown in Figure 5a. Apart from the C 1s peak only Sn and O_2 related core levels are detectable in the spectrum. The peaks at 488 eV and 496 eV can be assigned to the binding energy of Sn 3d electrons. A quantitative analysis based on the intensity of the spectral lines of Sn and O_2 (Figure.5b) gives the ratio of atomic percentage of O_2 to Sn as 1.4. This high O/Sn ratio favours the formation of acceptors V_{Sn}, which thus produces more mobile holes [15]. This observation is in accordance with the first principles calculation which suggests that the p-type conductivity of SnO films originate from the excess of oxygen or/and the tin vacancy [16].

A large deviation from the ideal stoichiometry observed due to metal vacancies results in the chemical formula $Sn_{1-\delta}O$. This nonstoichiometry is an intrinsic feature of this material and the metal vacancies cause a strain coupling which stabilizes the highly disordered nonstoichiometric phase. It has already been confirmed through compositional characterization, electron microscopy and diffraction studies that SnO is a nonstoichiometric phase with cation deficiency [17].

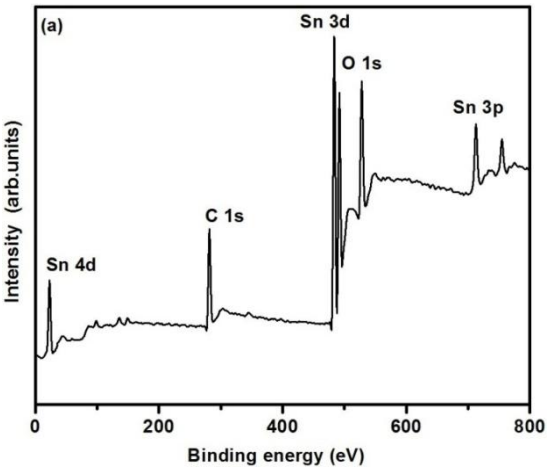

Figure 5a: XPS survey scan spectrum of SnO film

Apart from this possibility sometimes a high O/Sn ratio can also lead to SnO_2 phase formation in the film [18]. In that case free electron density in the film can become either approximately the same order of magnitude as the free holes or more than that leading to a highly resistive or an n -type film respectively. But in the present study the HRXRD pattern, Raman spectrum and energy gap value obtained from transmission spectrum ensures that the film is pure SnO and no SnO_2 phase has been formed.

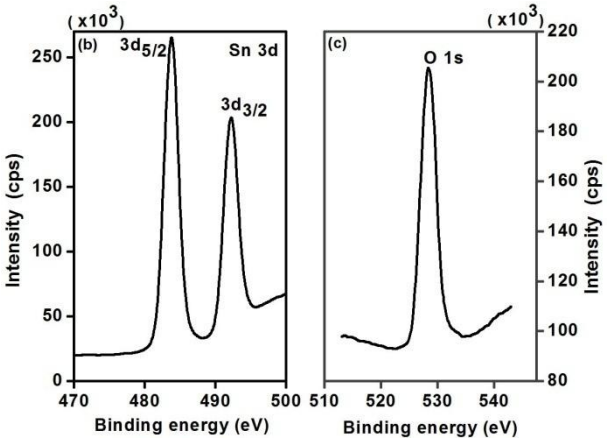

Figure 5b: XPS of Sn 3d and O 1s levels

III.3. Optical Properties

The SnO film is light yellowish in color and the transparency is less than 50% in the visible region [Figure 6]. The low transmission may be because of the presence of metallic tin in the film. There can be scattering loss also caused by the rough surface of the film. The thickness of the SnO film measured using stylus profiler is 200 nm. The direct band gap of the film calculated from the Tauc' plot (inset of figure 6) is 2.93 eV [8]. This value is much smaller than the optical band gap of SnO_2 (3.6 eV), substantiating GIXRD, Raman and XPS analysis.

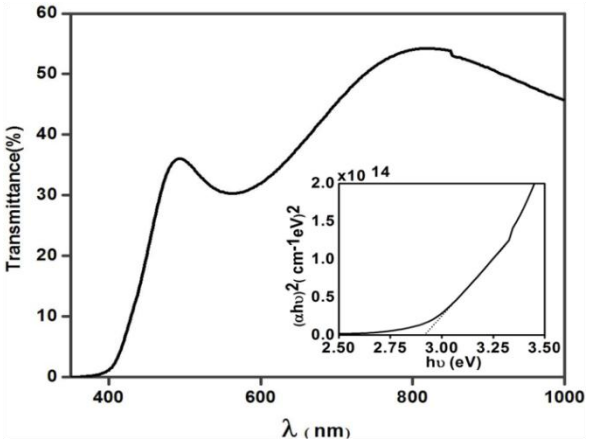

Figure 6: Transmission spectrum of SnO film; inset shows Tauc' plot

III.4. Electrical Properties

Electrical parameters like carrier concentration, carrier mobility and sheet resistance of the SnO film were measured using four point probe in the

van der Pauw configuration. The as deposited films were highly resistive. The SnO films exhibited p-type conduction with the mobility, hole concentration, and the resistivity in the range of 1.0-2.8 $cm^2V^{-1}s^{-1}$, 10^{15} to 10^{17} cm^{-3}, and 50−140 Ω cm, respectively. The carrier concentration and mobility of the films annealed at 200^0C could not be measured because of their high resistivity and limitation of the Hall-effect measurement system. High temperature (600^0C) annealed films where the majority carriers are electrons exhibited *n*-type conduction. On the basis of first-principle calculations [16], the p-type conductivity of SnO film originates more from the tin vacancy (V_{Sn}) rather than from oxygen interstitials (O_i). O_i and V_{Sn} are the defects with the lowest formation energy under O-rich conditions. The defect activation energies of V_{Sn} are estimated at ~ 0.1 eV from the VBM whereas O_i shows no defect level in the band gap. Therefore the existence of oxygen interstitials is expected not to contribute to the electric conductivity. On the other hand they drive down the formation energy of V_{Sn} and thereby favour the formation of shallower acceptor levels. The high level of oxygen in the film as found from the XPS analysis which is expected to be interstitial ones thus support the *p*- type conductivity. Previously also experimental results have verified the relation between the *p*-type conductivity and the degree of the off-stoichiometry in epitaxial SnO films [19]. However, there are reports where SnO film shows *p*-type conductivity only under perfect stoichiometric ratio [20]. They have attributed the improvement of film quality as a result of annealing as the explanation for this discrepancy. During the annealing process, an increase in grain size takes place, which reduces the carrier scattering from grain boundary, thereby giving rise to the improvement of carrier mobility and film conductivity.

III.5. Morphological Properties

Figure 7 shows the surface morphology of the annealed SnO film investigated by atomic force microscopy. The root mean square (RMS) surface roughness was found to be 19 nm. The grains are fused together compactly to form hillocks and clusters along the SnO film surface. During annealing process atoms rediffuse and migrate and the crystal grains grow along low stress directions, resulting in faceted surface and larger RMS roughness. The high energy of the particles in the ablation plume also can contribute to a high surface roughness.

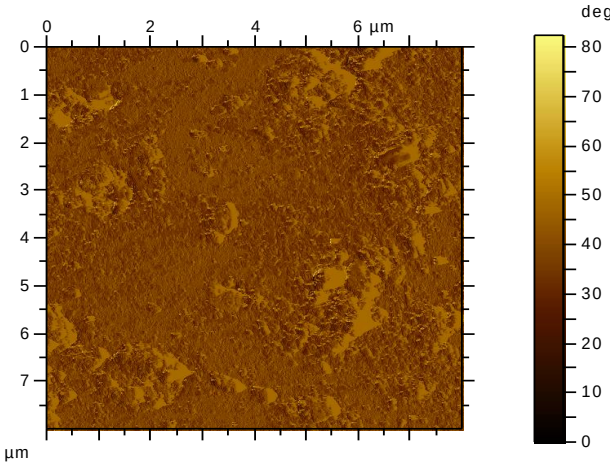

Figure 7: AFM image of SnO film

IV. CONCLUSIONS

In summary, polycrystalline *p*- type semiconducting SnO thin film was deposited successfully by the pulsed laser ablation of a metallic Sn target. From Hall measurements hole mobility ~1.0-2.8 $cm^2V^{-1}s^{-1}$, hole concentration ~ 10^{15} to 10^{17} cm^{-3}, and resistivity ~ 50−140 Ω cm, are obtained for different films. Sn vacancy is found to contribute for the p- type conductivity. Even the trivial variations in the deposition and annealing conditions lead to large variations in the concentration and mobility of holes in the film, as indicated by the range of values in the hall measurements. In the present work even though the values of carrier concentration and hole mobility were comparable to those previous reports suitable for p-type TFT application, we couldn't succeed in fabricating a TFT, mainly because of the non uniformity and surface roughness of the film.

Acknowledgement

The author gratefully acknowledges University Grants Commission, India for FIP fellowship.

REFERCNCES

[1] E. Fortunato, A. Gonçalves, A. Pimentel, P. Barquinha, G. Gonçalves, L. Pereira, I. Ferreira, R. Martin "Zinc oxide, a multifunctional material: from material to device applications", Applied Physics A, **96**, 197- 205 (2009).

[2] K. Nomura, H. Ohta, A. Takagi, T. Kamiya, M. Hirano, H. Hosono "Room-temperature fabrication of transparent flexible thin-film transistors using

amorphous oxide semiconductors", Nature, **432**, 488-492 (2004)

[3] Dhananjay, Chih-Wei Chu "Realization of In_2O_3 thin film transistors through reactive evaporation Process", Applied Physics Letters, **91**, 132111- 132111-3 (2007).

[4] H. Kawazoe, M. Yasukawa, H. Hyodo, M. Kurita, H. Yanagi, H. Hosono "P-type electrical conduction in transparent thin films of $CuAlO_2$", Nature **389**, 939-942 (1997).

[5] H.Yanagi, H. Kawazoe, A. Kudo, M. Yasukawa, H. Hosono "Chemical Design and Thin Film Preparation of p-Type Conductive Transparent Oxides", Journal of Electroceramics **4**, 407-414 (2000).

[6] M. A Myers, J. H. Lee, Z. Bi , H. Wang "High quality p-type Ag-doped ZnO thin films achieved under elevated growth temperatures", J. Phys. Condens. Matter **24**, 145802 (2012).

[7] Y. Ogo, H. Hiramatsu, K. Nomura, H. Yanagi, T. Kamiya, M. Hirano, H. Hosono "p-channel thin-film transistor using p-type oxide semiconductor, SnO" , Applied Physics Letters, **93**, 032113-032113-3 (2008).

[8] R. Sivaramasubramaniam. R. Muhamad, S. Radhakrishn "Optical Properties of Annealed Tin (II) Oxide in Different Ambients", Phys. Stat. Sol. (a), **136**, 215-222 (1993).

[9] Y. Ogo, H. Hiramatsu, K. Nomura, H.Yanagi, T. Kamiya, M. Kimura, M. Hirano, H. Hosono "Tin monoxide as an s-orbital-based p-type oxide semiconductor: Electronic structures and TFT application", Phys. Status Solidi A **206**, 2187-219 ,(2009).

[10] K.C. Sanal, M.K. Jayaraj "Growth and characterization of tin oxide thin films and fabrication of transparent p-SnO/n-ZnO p–n hetero junction, Materials Science and Engineering B **178**, 816-821 (2013).

[11] E. Fortunato, R. Barros, P. Barquinha, V. Figueiredo, S. H. K. Park "Transparent p-type SnOx thin film transistors produced by reactive rf magnetron sputtering followed by low temperature annealing", Applied Physics Letters, **97,** 052105-052105-3 (2010).

[12] H. Fan, S. A. Reid "Phase Transformations in Pulsed Laser Deposited Nanocrystalline Tin Oxide Thin Films", Chem. Mater.**1**, 564-567 (2003).

[13] J.Geurts, S.Rau, W.Richter, F.J. Schmitte "SnO films and their oxidation to SnO_2: Raman scattering,IR reflectivity and x-ray diffraction studies", Thin Solid Films, **121**, 217-225 (1984).

[14] R. S. Katiyars, P. Dawsons, M. M. Hargreaves, G. R. Wilkinson "Dynamics of the rutile structure 111.Lattice dynamics, infrared and Raman spectra of SnO_2", J. Phys. C: Solid St. Phys., **4,** 2421-2431 1971.

[15] W. Guo, L. Fu, Y. Zhang, K. Zhang, L. Y. Liang,Z. M. Liu, H. T. Cao, X. Q. Pan, "Microstructure, optical, and electrical properties of p-type SnO thin films", Applied Physics Letters, **96** , 042113-042113-3 (2010).

[16] A.Togo, F.Oba, I.Tanaka, K.Tatsumi "First-principles calculations of native defects in tin monoxide",Phys. Rev. B, **74** ,195128- 195128-8 (2006).

[17] M. S Moreno, A.Varela, L. C. OteroDiaz "Cation nonstoichiometry in tin-monoxide-phase $Sn_{1-\delta}O$ with tweed microstructure", Phys. Rev. B, **56**, 5186-5192 (1997).

[18] H. Yabuta,N. Kaji, R. Hayashi, H. Kumomi, K. Nomura, T. Kamiya, M. Hirano, and H. Hosono "Sputtering formation of p-type SnO thin-film transistors on glass toward oxide complimentary circuits", Applied Physics Letters **97**, 072111-072111-3 (2010).

[19] X.Q. Pan, L. Fu "Tin Oxide Thin Films Grown on the ($\bar{1}$012) Sapphire Substrate", Journal of Electroceramics, **7**, 35- 46 (2001).

[20] Ling Yan Liang, Zhi Min Liu, Hong Tao Cao, Xiao Qin Pan "Microstructural, Optical, and Electrical Properties of SnO Thin Films Prepared on Quartz via a Two-Step Method", Applied materials and interfaces, 2, 1060–1065 (2010).